

The Radiation Environment in and near High Gradient RF Cavities

J. Norem

HEP Division, Argonne National Laboratory, Argonne IL 60439

A. Moretti, M. Popovic

Fermi National Accelerator Laboratory, Batavia IL 60540

(Jan 31, 2000)

A. Cavity Parameters

Measurements of the X-ray flux, electron flux and spectrum are presented with the aim of evaluating the usefulness of ionization sensitive single particle detectors in the immediate environment of an RF cavity. The measured fluxes are found to be roughly consistent with field emission of electrons followed by one generation of bremsstrahlung photon production, with absorption and scattering of the final photons and electrons in the cavity and vacuum chamber structure.

I. INTRODUCTION

The production of x rays by rf cavities is well known [1] [2]. This x-ray flux generally represents a significant radiation dose and produces the requirement that rf cavities must be surrounded by thick concrete shielding during tune up and operation.

In muon cooling and other applications it has become desirable to consider using rf cavities near sensitive ionization detectors. The operation of single particle detectors near such cavities is difficult because the low energy electrons and x-rays can be both highly ionizing and penetrating, and could produce a troublesome background in detectors. This paper outlines the mechanism of x ray production in high energy cavities and presents measurements of the spectrum and scaling laws which should permit estimates of fluxes in cavities of different geometries.

II. X RAY PRODUCTION MECHANISMS

X ray production from rf cavities results from bremsstrahlung produced from dark current electrons hitting the body of the cavity and nearby solid components. This x-ray flux is then attenuated by both the production material and by transmission through any external structure. The electron flux would be influenced by low energy beam optics along the beam axis, however the x-rays could scatter and penetrate freely. Although many measurements of the overall x ray dose have been made as part of radiation protection and cavity conditioning programs, there has evidently been little need for specific knowledge of the spectrum of x rays produced or their dependence on cavity parameters.

The parameters of a range of cavities useful for muon cooling can be approximated by assuming that these cavities operate with a local electric field equal to some multiple, (perhaps 3), of the Kilpatrick limit, $E_k(f)$, for the appropriate frequency f . Assuming a reasonable cavity length, l , permits one to determine the optics of electrons, most of which cross the gap and gain a kinetic energy $E_e \sim 3E_k l$. The first line of the table gives the numbers for the cavity used in the test.

TABLE I, Cavity Parameters

f MHz	l m	$3E_k$ MV/m	E_e MeV	r_e cm
1300	0.02	96.6	2.4	0.19
805	0.06	78.6	4.2	0.33
400	0.15	58.5	8.2	0.65
200	0.30	44.4	12.5	1.00
70	0.80	30.0	22.1	1.75

The dark current electrons from single gap cavities and the x rays they produce tend to be comparatively low energy. At these low energies, the total electron track lengths (range), r_e , are important, since the ranges (at 0.13 - 1.3 radiation lengths) not large enough to permit development of an electromagnetic shower, but are large enough to produce bremsstrahlung at significant depths in a copper structure. These low energy electrons are usually described in terms of the critical energy, E_c , where the electron range equals one radiation length, and radiation and ionization energy loss terms are equal. In copper, this critical energy is 21.5 MeV, and the radiation length, L_R , is 1.43 cm. Dark current electrons which pass through many cells can have a much higher energy and may begin to have significant showers.

At low energies, showers are suppressed both by the small probability of bremsstrahlung, (roughly r_e/L_R) and the comparatively high photoelectric absorption coefficients for low energy photons, thus only the first generation of a shower would be expected to be significant.

B. Field Emission

Dark current electrons are produced by tunneling through the electrostatic potential at the surface of the

metal, first described by Fowler and Nordheim in 1928 [7] [8], and experimentally checked in 1953 [9]. The equation for the emitted current density, j , in A/m^2 is

$$j(E) = \frac{A_{FN}(\beta_{FN}E)^2}{\phi} \exp\left(-\frac{B_{FN}\phi^{3/2}}{\beta_{FN}E}\right),$$

where E is the electric field in MV/m, ϕ is the work function of the material in eV, with $A_{FN} = 1.54 \times 10^6$, $B_{FN} = 6830$, and β is a term that expresses the enhancement of the local electric field at the presumeably pointlike emitter compared with the average electric field at the surface. In principle βE can be a high multiple of the average electric field E . The electrons produced by this mechanism could be amplified by multipactoring.

C. Electron Bremsstrahlung

The spectrum of photons, $\Phi(E_0, \nu)$, emitted by low energy, (~ 1 MeV), electron bremsstrahlung, with no atomic shielding, is described by the relation [3] [4]

$$\Phi d\nu = C \frac{d\nu}{\nu} 4 \left[1 + \left(\frac{E}{E_0} \right)^2 - \frac{2E}{3E_0} \right] \left(\log \frac{2E_0E}{mc^2 h\nu} - 0.5 \right),$$

with $C = (Z^2/137)(e^2/mc^2)^2$. The angular distribution is approximately

$$\frac{d\sigma}{d\omega} \sim [\sin(\theta/2)]^{-4},$$

which is similar to Rutherford scattering. Electrons of this low energy are moving somewhat isotropically through the copper because multiple scattering angles for copper are very large.

D. Photon Absorption

Low energy photons are scattered and absorbed in materials. For small emittance beams in good geometry configurations an exponential absorption of x ray photons describes attenuation,

$$N(x) = N_0 e^{-\mu x},$$

where the mass absorption coefficient μ is a function of photoelectric, compton and pair production cross sections. The absorption coefficients for different materials are tabulated as a function of energy in a number of sources [5] [6]. This parameterization of attenuation is not accurate, however, if the scattered photons or recoil electrons are considered, since the secondary photons, neglected in the exponential absorption, can carry most of the energy of the primary photon. Thus most problems are usually solved by Monte Carlo methods.

III. MEASUREMENTS

The radiation fluxes were measured using the absorber method, where a range of of absorbers in a “good” geometry were used to filter the radiation before it hit the detectors. The fluxes were measured with thermoluminescent detectors (TLD’s) [11], which have the desirable features that they have a flat detection efficiency over a very large range of dose, and a sensitivity which is independent of the photon energy. The detector, shown in Figure 1, uses lead collimators to separate the fluxes through different apertures. While the TLD’s provided a very large dynamic range and good sensitivity, the readout required at least one day, which complicated the analysis.

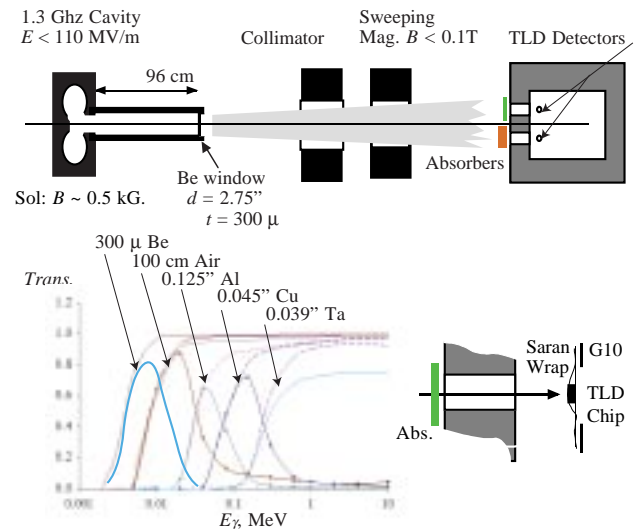


FIG. 1. The apparatus used for the x ray spectrum measurements.

The cavity used was a 1.3 GHz rf electron gun built by the Taiwan Synchrotron source [12]. This gun can be operated at a comparatively high electric field of 130 MV/m surface field. A thin, (300 μm), Beryllium window was used in the forward direction to transmit a minimally attenuated x-ray flux forward to the detectors. A sweeping magnet permitted measurements of the electron component of the beam. The detector, had five absorber/detector cells separated by 4 cm. A similar detector was used at 90 degrees to measure the flux transmitted by the cavity walls at large angles. The spectrum was produced by subtracting the dose from detectors with different absorbers, and assuming the mean energy of the part of the spectrum that was isolated. Measurements at two angles were not made at the same time.

Radiation doses measure absorbed energy and, for electrons and photons which have radiation weighting factor $w_R = 1$, with 1 sievert = 1 gray = 1 joule/kg, with 1 rad = 1 rem = 0.01 gray [10]. For low energy electrons and photons, these produce the relations:

$$\text{Dose [rem/h]} = 1.6 \times 10^{-6} \Phi_\gamma [\text{MeV cm}^{-2}\text{s}^{-1}],$$

and

$$\text{Dose [rem/h]} \sim 1.6 \times 10^{-4} \Phi_e [\text{electrons cm}^{-2}\text{s}^{-1}].$$

The calculated radiation flux, in photons/cm²/pulse, at zero and 90 degrees are shown in Figures 2 and 3, assuming all the radiation dose is due to photons. At higher energies the data are consistent with the spectrum produced by the EGS4 Monte Carlo, described below, but at low energies, both small and large angles show a significant excess due to the electron component which has both short range and higher ionization. The normalization of the Monte Carlo results is the same in Figures 2, 3 and 6 to permit easy comparison of the data. The low energy component was sensitive to the field in the sweeping magnet, whereas the high energy component was not.

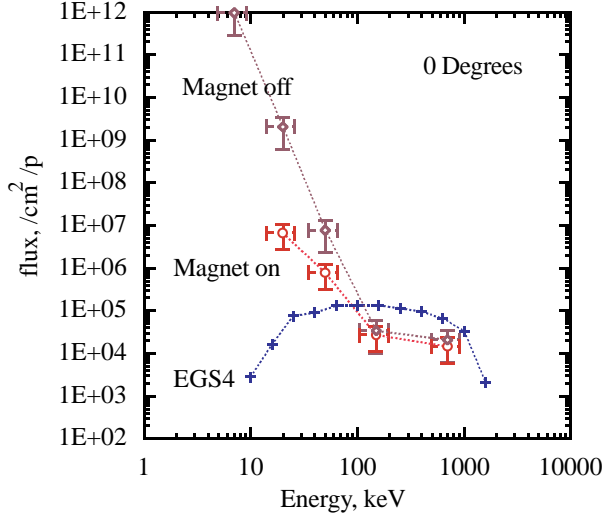


FIG. 2. X ray flux at zero degrees.

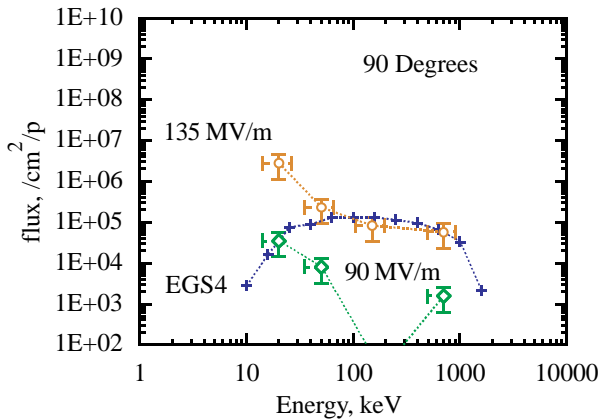


FIG. 3. X ray flux at 90 degrees.

The electric field dependence of the radiation was measured both by placing a SmartION [13] dosimeter near

the cavity and by measuring the spectrum with TLD's and absorbers. These measurements were primarily done at 90 degrees to the cavity axis. The results using the dosimeter are shown in Figure 4, fitted to a curve of the form $D \propto E^{9.6}$ to show the dependence on electric field E . The $E^{9.6}$ dependence on electric field is common at many facilities, and was seen during the tuneup of LEP cavities in CERN [2].

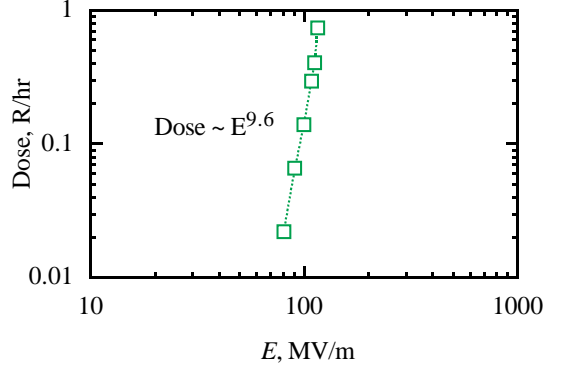


FIG. 4. Dose rate as a function of RF field at 90 degrees from the axis.

Since the dark current backgrounds are large, it is desirable to understand how uniformly the electron and x-ray fluxes were distributed from pulse to pulse and within the rf pulse length. (Uniform backgrounds would be easier to subtract.) We intend to continue taking data with an 805 MHz 5 cell cavity running at somewhat lower electric fields.

IV. ANALYSIS

The program EGS4 [14] was used to simulate the production spectrum for low energy photons from electrons of a few MeV. Typical results for electrons on copper are shown in Figure 5, which shows the angular and energy distribution of secondary photons from low angle 2 MeV electrons. The angular distribution is roughly flat, as is the energy distribution on a semi-log axis. The upper limit on photon energy is given by the bremsstrahlung spectrum for the 2 MeV electrons, and the lower energy is given by the absorption of these photons in the copper. The comparatively flat angular distribution is due partially to the large multiple scattering experienced by low energy electrons. These simulations were used to compare the data taken in Figures 2, 3 and 6.

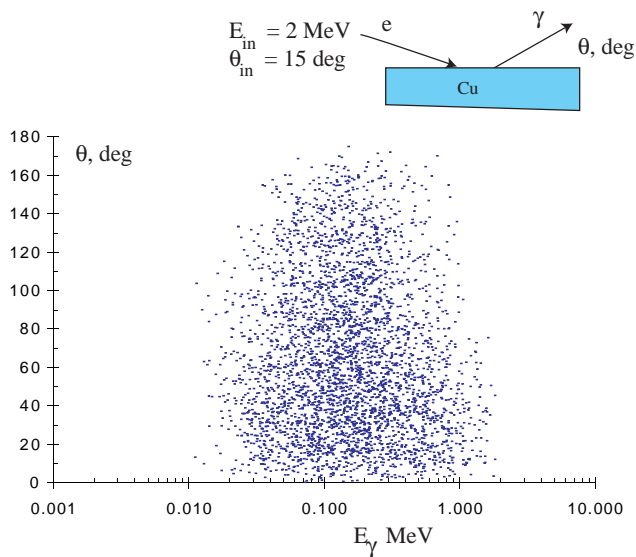


FIG. 5. EGS4 predictions of secondary photons.

When the low energy data points in Figure 2 are re-analysed assuming that the low energy signal is composed primarily of electrons, and the detectors operate as a range telescope, one obtains results like those in Figure 6, which show an intense local flux of electrons on axis which can produce significant radiation doses. Since the absorber geometry was optimized for low emittance photon beams rather than low energy electrons the analysis assuming electron ranges introduces some systematic errors. The spectrum shape is changed because a given radiation dose is produced by a lower flux of electrons than photons, and a correction must be made for electrons which have multiple scattered out of the beam.

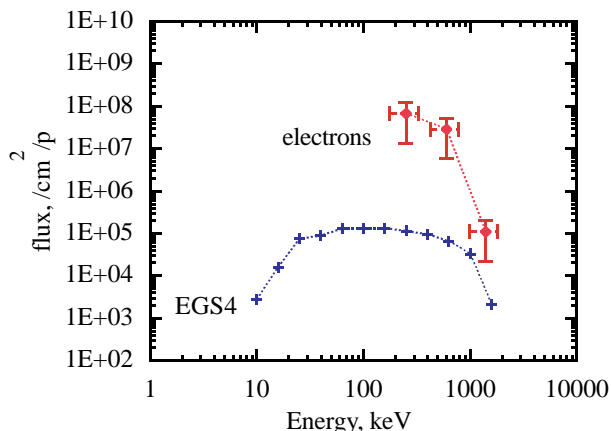


FIG. 6. Measurements of the dark current spectrum.

A. General Applicability

In principle, radiation fluxes measured for one cavity might not be generally applicable since cavities operate under a variety of conditions. One can, however, calculate the local flux of photons and electrons approximately from the radiation level measured outside the shielding, and then multiply this by the attenuation factor in the shielding, giving the total flux of photons in the cavity region. At low energy, where the fluxes are somewhat isotropic, $n_\gamma = 4\pi R^2 \phi_\gamma$, which is produced by n_e dark current electrons, where $n_e = (r_e/L_R)n_\gamma$, giving an instantaneous current of $I_d = qn_e/\Delta t$, where Δt and q are the rf pulse length and electron charge. We assume that this current can produce electrical breakdown by means of a thermal avalanche, and this avalanche process will be fairly similar from one cavity to another.

B. Minimizing Dark Currents and X-Rays

The two methods of reducing the dark current and x-ray fluxes are to reduce the electric field near the surface which should reduce the flux by a factor like $E^{9.6}$, (as shown in Figure 4), and to treat the surface chemically to minimize dark current production, which should also have a significant effect. Coatings such as TiN, CaF and CaN have been considered [15], in addition to many of the techniques used for superconducting cavities [8]. In addition it seems desirable to decrease the resolution time, since the dark current and x-ray signal should be proportional to the resolution time.

V. CONCLUSIONS

The x-ray and dark current fluxes from rf cavities can limit the performance of ionization sensitive detectors placed near them. It may be possible to reduce these fluxes by use of lower electric fields and/or different surface treatments on the rf surfaces and reducing the resolving time of the detectors should reduce the background by about the same amount. This program will continue using an 805 MHz cavity at Fermilab.

VI. ACKNOWLEDGMENTS

This work was supported by the U. S. Department of Energy, Office of High Energy Physics. W. Gai and M. Conde of ANL/HEP, T. Leveling of FNAL/rad safety, G. Geschonke and E. Keil of CERN, S. Henderson of Cornell, and Elwin Dolochek of ANL Health Physics have been very helpful.

- [1] E. McCrory, *The Commissioning and Initial Operation of the Fermilab 400 MeV Linac*, Proceedings of the 1994 Linac Conference, (1994), 36.
- [2] M. Silari, S. Agosteo, J. C. Gaborit, L. Ulrici, Nucl. Instrum. Methods Phys. Res. A, 432 (1999) 1
- [3] H. A. Bethe and J. Ashkin, *Passage of Radiations Through Matter*, in *Experimental Nuclear Physics* E. Segre, ed., John Wiley & Sons, Inc. New York, 1953, p166.
- [4] F. Sauter, Ann. Physik, **20** (1934) 404
- [5] O. I. Leipunskii, B. V. Novozhilov, V. N Sakharov, *The Propagation of Gamma Quanta in Matter*, Pergamon Press, Oxford, 1965.
- [6] <http://www-pdg.lbl.gov/2000/passagerpp.pdf>
- [7] R. H. Fowler and L. Nordheim, Proc. Roy Soc **A119** 173 (1928)
- [8] H. Padamsee, J. Knobloch, T. Hays, *RF Superconductivity for Accelerators*, John Wiley and Sons, Inc, New York, 1998
- [9] W. P. Dyke, and J. K. Trolan, Phys. Rev. **89** (1953) 799
- [10] W. P. Swanson, *Radiological Safety Aspects of the Operation of Electron Linear Accelerators*, IAEA Technical Reports Series No. 188, IAEA, Vienna, 1979
- [11] G. Shani, *Radiation Dosimetry Instrumentation and Methods*, CRC Press, Boca Raton, 1991
- [12] C. H. Ho, SRRC, Hsinchu, Taiwan, Private Communication
- [13] Perspective Scientific Limited, W1M 1LA, England
- [14] <http://ehssun.lbl.gov/egs/egs.html>
- [15] R. Silbergliitt, FM Technologies, Farifax VA, Private Communication.